

Steady-state molecular dynamics simulation of vapour to liquid nucleation with McDonald's dæmon

Martin Horsch, Svetlana Miroshnichenko and Jadran Vrabec¹

Universität Paderborn, Institut für Verfahrenstechnik, Warburger Str. 100, 33098 Paderborn, Germany

Abstract. The most interesting step of condensation is the cluster formation up to the critical size. In a closed system, this is an instationary process, as the vapour is depleted by the emerging liquid phase. This imposes a limitation on direct molecular dynamics (MD) simulation of nucleation by affecting the properties of the vapour to a significant extent so that the nucleation rate varies over simulation time. Grand canonical MD with McDonald's dæmon is discussed in the present contribution and applied for sampling both nucleation kinetics and steady-state properties of a supersaturated vapour.

The idea behind that approach is to simulate the production of clusters up to a given size for a specified supersaturation. In that way, nucleation is studied by a steady-state simulation. A series of simulations is conducted for the truncated and shifted Lennard-Jones fluid which accurately describes the fluid phase coexistence of noble gases and methane. The classical nucleation theory is found to overestimate the free energy of cluster formation and to deviate by two orders of magnitude from the nucleation rate below the triple point at high supersaturations.

Keywords: Non-equilibrium statistical mechanics, nucleation, molecular dynamics

PACS: 05.70.Ln, 64.70.F-, 36.40.Sx

INTRODUCTION

The key properties of nucleation processes in a supersaturated vapours are the height $\Delta\Omega^*$ of the free energy barrier that must be overcome to form stable clusters and the nucleation rate \mathcal{J} that indicates how many macroscopic droplets emerge in a given volume per time. The most widespread approach for calculating these quantities is the classical nucleation theory (CNT) [1], which has significant shortcomings, e.g., it overestimates the free energy of cluster formation [2, 3]. An important problem of CNT in case of vapour to liquid nucleation is that the underlying basic assumptions for the liquid do not apply to nanoscopic clusters [4–6].

Molecular simulation permits the investigation of nanoscopic surface effects and the stability of supersaturated states from first principles, using effective pair potentials. For instance, the spinodal line can be detected with Monte Carlo (MC) [7] simulation methods; in experiments, it can only be approximated as it is impossible to discriminate an unstable state from a metastable state where $\Delta\Omega^*$ is low. Equilibria [8] and vapourization

¹ Author to whom correspondence should be addressed: Prof. Dr.-Ing. habil. J. Vrabec. E-mail: jadran.vrabec@upb.de.

processes [9, 10] of single clusters can also be simulated to obtain the surface tension as well as heat and mass transfer properties of strongly curved interfaces. Moreover, molecular dynamics (MD) [11–13] and MC [14] simulation of supersaturated systems with a large number of particles are useful for the study of very fast nucleation processes, whereas lower nucleation rates can be calculated by transition path sampling based methods [15, 16].

Equilibrium simulations fail to reproduce kinetic properties of nucleation processes such as the overheating of growing clusters due to latent heat. On the other hand, direct MD simulation of nucleation, where cluster formation is observed directly in a near-spinodal supersaturated vapour, has its limits: if nucleation occurs too fast, it affects the properties of the vapour to a significant extent so that the nucleation rate obtained according to the method of Yasuoka and Matsumoto [11] and other properties of the system vary over simulation time [17]. In the present work, nucleation is studied as a steady-state process by combining grand canonical MD (GCMD) and McDonald’s dæmon [18, 19], an ‘intelligent being’ that eliminates large droplets from the system.

SIMULATION METHOD

Supersaturated states can be characterized in terms of the difference between the chemical potential μ of the vapour and the saturated chemical potential $\mu_\sigma(T)$. The chemical potential of the vapour can be regulated by simulating the grand canonical ensemble with GCMD: alternating with canonical ensemble MD steps, particles are inserted into and deleted from the system probabilistically, with the usual grand canonical acceptance criterion [20]. For a test insertion, random coordinates are chosen for an additional particle, and for a test deletion, a random particle is removed from the system. The potential energy difference $\Delta\mathcal{V}$ due to the test action is determined and compared with the chemical potential. The acceptance probability for insertions is

$$\mathcal{P} = \min \left(1, \exp \left[\frac{\mu - \Delta\mathcal{V}}{k_B T} \right] \frac{V}{\Lambda^3(N+1)} \right), \quad (1)$$

while for deletions it is

$$\mathcal{P} = \min \left(1, \exp \left[\frac{-\mu - \Delta\mathcal{V}}{k_B T} \right] \frac{V}{\Lambda^3 N} \right), \quad (2)$$

wherein Λ is the thermal wavelength. Of course, care must be taken that the momentum of the inserted particles is consistent with the simulated ensemble and does not introduce any artificial velocity gradients. The MD integration time step was $\Delta t = 0.00404$ in reduced time units, i.e., $\sigma(m/\varepsilon)^{1/2}$, wherein ε is the energy parameter of the fluid model and m is the mass of a particle. The number of test actions per simulation time step was chosen between 10^{-6} and $10^{-3} N$, a value which was occasionally decreased after equilibration if very low nucleation rates were observed.

Molecular simulation of nucleation has to rely on a cluster criterion to distinguish the emerging liquid from the surrounding supersaturated vapour [21]. In the present case, the Stillinger criterion [22] was used to define the liquid phase and clusters were determined

as biconnected components. Whenever a cluster exceeded the specified threshold size Θ , an intervention of McDonald's dæmon removed it from the system, leaving a vacuum behind [18, 19].

NUCLEATION THEORY

The free energy of cluster formation is the same for the grand canonical and the isothermal-isobaric ensemble [23]. At specified values of the chemical potential μ of the supersaturated vapour, the total system volume V and the temperature T , it is related to the surface energy η by [24]

$$\Delta\Omega_v = \int_{V_\ell(1)}^{V_\ell(v)} (p - p_\ell) dV_\ell + \int_{\mathcal{F}(1)}^{\mathcal{F}(v)} \left(\frac{\partial \eta}{\partial \mathcal{F}} \right) d\mathcal{F} + \int_1^v (\mu_\ell - \mu) dv, \quad (3)$$

where v is the number of particles in the cluster, p is the supersaturated vapour pressure, $V_\ell(v)$ is the volume and $\mathcal{F}(v)$ the surface area of a cluster containing v particles. Note that μ_ℓ as well as p_ℓ are the chemical potential and the pressure of the liquid phase at the conditions prevailing inside the cluster. In CNT, it is assumed that the bulk liquid density at saturation ρ' and the density of a nanoscopic cluster are the same and all clusters are treated as spheres, i.e., $\rho_\ell = \rho'$ and $\mathcal{F}(v) = \mathcal{F}_\bullet(v) = (6\sqrt{\pi}v/\rho')^{2/3}$. Accordingly, the chemical potential of the liquid inside the nucleus is approximated by

$$\mu_\ell = \mu_\sigma(T) + \int_{p_\sigma}^{p_\ell} \frac{dp}{\rho_\ell} \approx \mu_\sigma(T) + \frac{p_\ell - p_\sigma(T)}{\rho'}, \quad (4)$$

and the cluster surface tension $\tilde{\gamma} = (\partial\eta/\partial\mathcal{F})$ by the surface tension γ of the planar vapour-liquid interface, leading to [25, 26]

$$d\Omega = \left[\gamma \sqrt[3]{\frac{2\pi}{3v} \left(\frac{4}{\rho'} \right)^2} + \mu_\sigma(T) - \mu + \frac{p - p_\sigma(T)}{\rho'} \right] dv. \quad (5)$$

The free energy of formation has a maximum $\Delta\Omega^*$ which lies at the size v^* of the critical nucleus. Including the Zel'dovič factor f_Z and the thermal non-accomodation factor $f_{\Delta T}$ of Feder *et al.* [1], the nucleation rate is

$$\mathcal{J} = f_{\Delta T} f_Z \frac{N_1}{V} \exp(-\beta\Delta\Omega^*) \frac{p\Lambda}{h} \mathcal{F}(v^*), \quad (6)$$

where N_1 is the number of vapour molecules in the system and h is the Planck constant.

Instead of using the surface tension of the planar interface, Laaksonen, Ford, and Kulmala (LFK) [27] proposed an expression equivalent to

$$\int_0^{\mathcal{F}(v)} \tilde{\gamma} d\mathcal{F} = \gamma \mathcal{F}(v) \left(1 + \alpha_1 v^{-1/3} + \alpha_2 v^{-2/3} \right). \quad (7)$$

The two parameters α_1 and α_2 are determined from the assumption that almost all particles are arranged either as monomers or as dimers and that the Fisher [28] equation

of state correctly relates p/T to the number of monomers and clusters present per volume. Effectively, LFK theory modifies CNT only by the introduction of the parameter α_1 , since α_2 cancels out for all free energy differences if the usual assumption $\mathcal{F} \sim v^{2/3}$ is applied.

The Hale scaling law (HSL) is based on a different approach [29]. In agreement with experimental data on nucleation of water and toluene [29], it predicts

$$\mathcal{J} \sim \rho^{-2/3} \left(\frac{\gamma}{T} \right)^{1/2} p^2 \exp \left[\frac{4\gamma^3}{27(\ln S)^2} \right], \quad (8)$$

with a proportionality constant depending only on properties of the critical point.

In the present work, these theories are evaluated using Gibbs-Duhem integration over the metastable part of the vapour pressure isotherm collected by canonical ensemble MD simulation of small systems. The fluid model under consideration is the truncated and shifted Lennard-Jones (t. s. LJ) potential with a cutoff radius of 2.5σ [30]. Note that the chemical potential supersaturation, i.e., $S = \exp(\beta[\mu - \mu_\sigma(T)])$, deviates considerably from the pressure supersaturation p/p_σ and the density supersaturation ρ/ρ_σ , with respect to the saturated vapour pressure $p_\sigma(T)$ and density $\rho''(T)$ of the bulk, cf. Fig. 1. For the saturated chemical potential of the t. s. LJ fluid, a correlation based on previously published data [8] gives

$$\frac{\mu_\sigma(T) - \mu_{id}(T)}{k_B T} = -0.2367 - \frac{1.7106\epsilon}{k_B T} - \frac{1.1514\epsilon^2}{(k_B T)^2}. \quad (9)$$

In Fig. 2, the chemical potential supersaturation is shown as a function of the vapour density determined by GCMD simulation with McDonald's *dæmon*. These values agree well with the metastable vapour pressure isotherm of the t. s. LJ fluid obtained by canonical ensemble simulation.

INTERVENTION RATE AND NUCLEATION RATE

The size evolution of any given cluster can be considered as a random walk over the order parameter v , changing only by relatively small amounts Δv , usually by the absorption or emission of monomers. As discussed by Smoluchowski [31, 32] during his scientifically most productive period in L'viv and Kraków, the probabilities for the growth and decay transitions are proportional to the respective values of the partition function W , resulting in

$$\mathcal{P}^+(v) = \frac{1}{2} + \frac{(dW/dv)\Delta v}{2W + \mathcal{O}(v^2)} + \mathcal{O}(v^2), \quad (10)$$

and

$$\mathcal{P}^-(v) = \frac{1}{2} - \frac{(dW/dv)\Delta v}{2W + \mathcal{O}(v^2)} + \mathcal{O}(v^2). \quad (11)$$

The probability $\mathcal{P}^F(v)$ that a certain size is *eventually* reached (at any time during the random walk process), given that the current size is v , has the property

$$\mathcal{P}^F(v) = \mathcal{P}^+(v)\mathcal{P}^F(v + \Delta v) + \mathcal{P}^-(v)\mathcal{P}^F(v - \Delta v). \quad (12)$$

By substituting

$$\mathcal{P}^F(v \pm \Delta v) = \mathcal{P}^F(v) \pm \frac{d\mathcal{P}^F}{dv}\Delta v + \frac{d^2\mathcal{P}^F}{2dv^2}\Delta v^2 + \mathcal{O}(\Delta v^3), \quad (13)$$

it follows for small Δv neglecting terms of third order and beyond, that

$$\frac{dW}{Wdv} = \frac{-d(d\mathcal{P}^F/dv)}{2(d\mathcal{P}^F/dv)dv}. \quad (14)$$

Using the partition function for the grand canonical ensemble, the derivative of the probability is given by

$$\frac{d\mathcal{P}^F}{dv} = F \exp(2\beta\Delta\Omega_v), \quad (15)$$

where F is an integration constant. Obtaining the two remaining parameters from the boundary conditions

$$q_1 = 0, \quad (16)$$

$$\lim_{\Theta \rightarrow \infty} q_\Theta = 1, \quad (17)$$

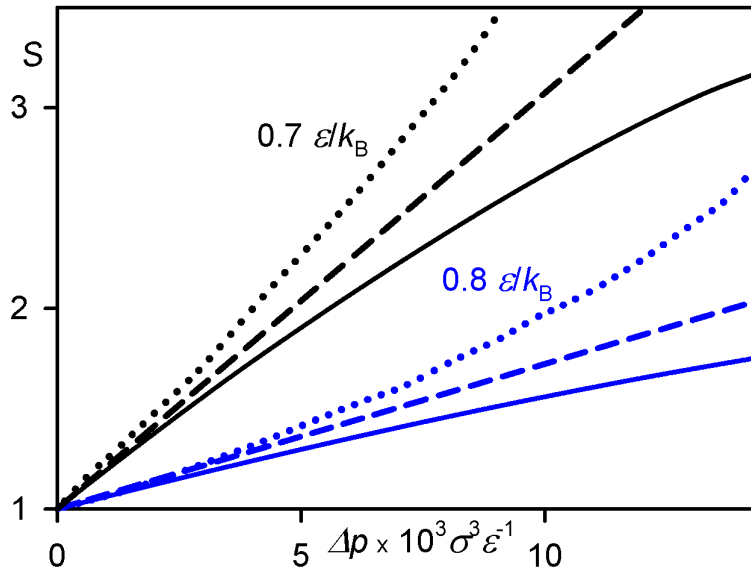


FIGURE 1. Chemical potential supersaturation S (—), pressure supersaturation p/p_σ (---), and density supersaturation ρ/ρ_σ (· · ·) in dependence of the excess pressure $\Delta p = p - p_\sigma$ at $T = 0.7$ and $0.8 \epsilon/k_B$.

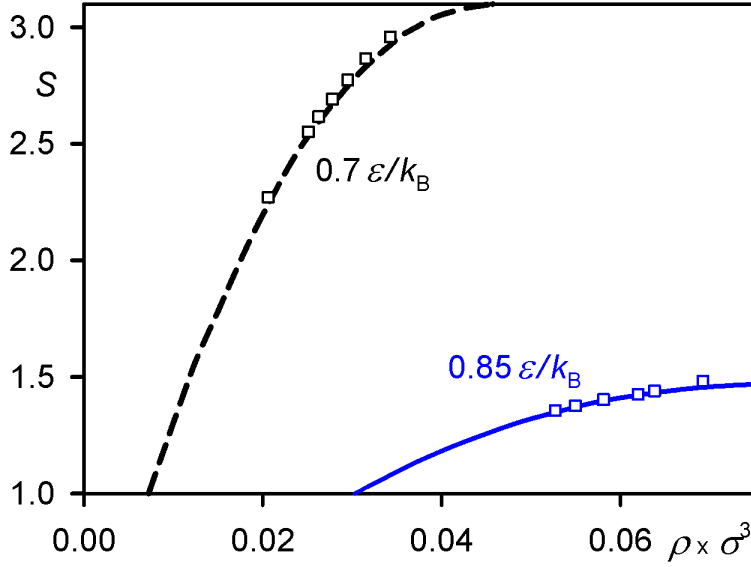


FIGURE 2. Density dependence of the chemical potential supersaturation for the vapour of the t. s. LJ fluid, obtained from GCMC simulation with McDonald’s dæmon (\square) and by integration of the Gibbs-Duhem equation using data from canonical ensemble MD simulation with $T = 0.7$ (---) and $0.85 \epsilon/k_B$ (—).

the probability q_Θ for a cluster containing Θ molecules of eventually reaching macroscopic size, i.e., $\mathcal{J} \rightarrow \infty$, is

$$q_\Theta = \frac{\int_1^\Theta \exp(2\beta\Delta\Omega_v) dv}{\int_1^\infty \exp(2\beta\Delta\Omega_v) dv}. \quad (18)$$

The intervention rate \mathcal{J}_Θ of McDonald’s dæmon is related to the nucleation rate \mathcal{J} by

$$\mathcal{J} = \mathcal{J}_\Theta q_\Theta. \quad (19)$$

Thus, with an intervention threshold far below the critical size, the intervention rate is many orders of magnitude higher the steady-state nucleation rate. However, as confirmed by the present simulation results shown in Tab. 1, it reaches a plateau for $\Theta > v^*$, where $v^* = 41$ according to CNT and 39 according to SPC.

RESULTS AND DISCUSSION

Homogeneous nucleation of the t. s. LJ fluid was studied by a series of GCMC simulations with McDonald’s dæmon for systems containing up to 17 million particles.

After a temporal delay, depending on the threshold size, the pressure and the intervention rate reached a constant value, cf. Fig. 3. In a canonical ensemble MD simulation under similar conditions as the GCMC simulation that is also shown in Fig. 3, the pressure supersaturation decreased from about 3 to 1.5 and the rate of formation was significantly lower for larger nuclei, due to the free energy effect accounted for by Eqs. (18) and (19) as well as the depletion of the vapour [19].

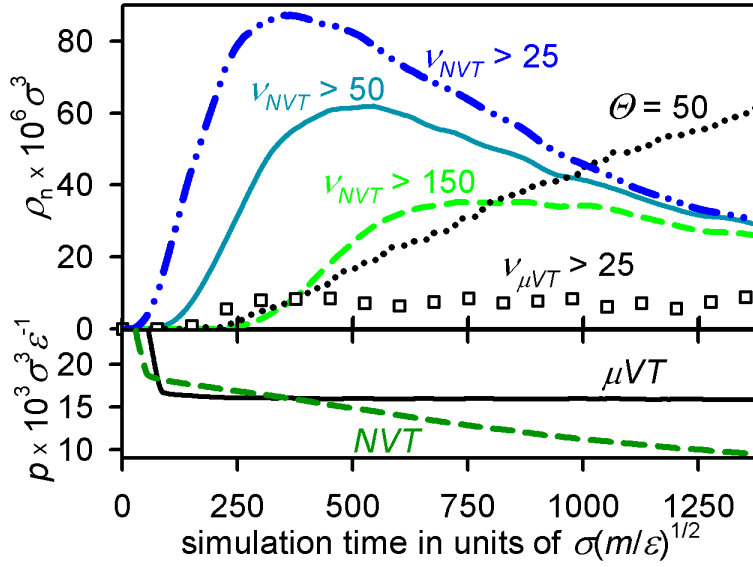


FIGURE 3. Top: Number per unit volume ρ_n of clusters containing more than 25 ($\cdot - \cdot$), 50 ($—$), and 150 ($- -$) particles in a canonical ensemble MD simulation at $T = 0.7 \epsilon/k_B$ and $\rho = 0.004044 \sigma^{-3}$ using a hybrid geometric-energetic cluster criterion, number per unit volume ρ_n of clusters with $v \geq 25$ (\square) in a GCMD simulation with $T = 0.7 \epsilon/k_B$, $S = 2.8658$, and $\Theta = 50$, using the Stillinger [22] cluster criterion with clusters determined as biconnected components, as well as the aggregated number of McDonald's daemon interventions per unit volume in the GCMD simulation, over simulation time. Bottom: Pressure over simulation time for the canonical ensemble MD simulation ($- -$) and the GCMD simulation with McDonald's daemon ($—$) [19].

The constant supersaturation of the GCMD simulation agreed approximately with the time-dependent supersaturation in the canonical ensemble about $t = 400$ after simulation onset, cf. Fig. 3. At this stage, the number of small clusters present per volume was similar in both cases, and the rate of formation for clusters with $v > 150$ at $t = 400$ in the canonical ensemble simulation was of the same order of magnitude as the intervention rate of the daemon.

TABLE 1. Dependence of the intervention rate \mathcal{J}_Θ as well as the probability q_Θ according to CNT and LFK on the intervention threshold size Θ for McDonald's daemon during GCMD simulation at $T = 0.7 \epsilon/k_B$ and $S = 2.4958$, where the rates are given in units of $(\epsilon/m)^{1/2} \sigma^{-4}$. The number of particles in the system and the values for the pressure supersaturation p/p_σ refer to the steady state and the constant volume of the system is given in units of σ^3 .

V	N	p/p_σ	Θ	$\ln q_\Theta(\text{CNT})$	$\ln q_\Theta(\text{LFK})$	$\ln \mathcal{J}_\Theta$
5.38×10^6	124000	2.70	10	-16.7	-12.7	-13.6
4.32×10^7	1020000	2.75	20	-8.14	-6.33	-17.0
5.38×10^6	129000	2.78	25	-5.55	-4.34	-17.6
5.38×10^6	129000	2.78	35	-2.32	-1.82	-19.9
4.32×10^7	1040000	2.78	48	-0.508	-0.400	-21.7
4.32×10^7	1040000	2.78	65	-0.022	-0.019	-21.9
2.15×10^7	518000	2.77	74	-0.002	-0.002	-22.1

Van Meel *et al.* [16] determined by MC simulation with forward flux sampling that supersaturated vapours of the t. s. LJ fluid at a temperature of $T = 0.45 \epsilon/k_B$, i.e., significantly below the triple point $T_3 = 0.65 \epsilon/k_B$, initially undergo vapour to liquid nucleation, and CNT is known to underestimate the vapour to liquid nucleation rate of unpolar fluids [13]. The present daemon intervention rates confirm this conclusion. LFK and HSL are significantly more accurate than CNT. Note that in Tab. 2, the nucleation rate according to Eq. (19) based on the CNT value of q_Θ is given.

From Tab. 2 it is also confirmed that the ‘direct observation method’ (DOM) [17], which in the present case corresponds to assuming

$$\ln \mathcal{J}_\Theta = \ln \mathcal{J} - \ln q_\Theta = -\ln \tau V, \quad (20)$$

where τ is the temporal delay of formation for the first sufficiently large cluster, is inadequate for nucleation near the spinodal line.

CONCLUSION

GCMD with McDonald’s daemon was established as a method for steady-state simulation of nucleating vapours at high supersaturations. A series of simulations was conducted for the t. s. LJ fluid. CNT was found to underpredict the nucleation rate below the triple point, whereas LFK and HSL more accurately describe vapour to liquid nucleation of the t. s. LJ fluid.

ACKNOWLEDGMENTS

The authors would like to thank G. Chkonia, H. Hasse, S. Sastry, C. Valeriani, and J. Wedekind for fruitful discussions and Deutsche Forschungsgemeinschaft for funding SFB 716. The presented research was conducted under the auspices of the Boltzmann-Zuse Society of Computational Molecular Engineering (BZS), and the simulations were performed on the HP XC4000 supercomputer at the Steinbuch Centre for Computing, Karlsruhe, under the grant LAMO, as well as the *phoenix* supercomputer at Höchstleistungsrechenzentrum Stuttgart (HLRS) under the grant MMHBF.

TABLE 2. Vapour to liquid nucleation rate at $T = 0.45 \epsilon/k_B$ from GCMD simulation with McDonald’s daemon. The theories were evaluated with respect to the metastable vapour-liquid equilibrium at $p_\sigma = 4.28 \times 10^{-5} \epsilon/\sigma^3$ [16], and the vapour-liquid surface tension $\gamma = 1.07 \epsilon/\sigma^2$ [16] was used.

p/p_σ	$10^{-6}N$	Θ	$-\ln \tau V$	$\ln q_\Theta(\text{CNT})$	$\ln \mathcal{J}$	$\ln \mathcal{J}_{\text{CNT}}$	$\ln \mathcal{J}_{\text{LFK}}$	$\ln \mathcal{J}_{\text{HSL}}$
30.2	0.397	9	-23.1	-4.57	-26.4	-31.5	-26.2	-24.7
32.4	0.429	9	-23.0	-3.80	-25.0	-30.5	-25.4	-24.0
55.9	1.07	12	-22.5	-0.062	-18.0	-24.2	-20.2	-19.5
74.7	17.1	24	-17.1	≈ 0	-18.8	-21.8	-18.6	-17.7

REFERENCES

1. J. Feder, K. C. Russell, J. Lothe, and G. M. Pound, *Adv. Phys.* **15**, 111–178 (1966).
2. V. Talanquer, *J. Phys. Chem. B* **111**, 3438–3446 (2007).
3. B. Chen, H. Kim, S. J. Keasler, and R. B. Nellas, *J. Phys. Chem. B* **112**, 4067–4078 (2008).
4. R. C. Tolman, *J. Chem. Phys.* **17**, 333–337 (1949).
5. L. S. Bartell, *J. Phys. Chem. B* **105**, 11615–11618 (2001).
6. K. Katsov and J. D. Weeks, *J. Phys. Chem. B* **106**, 8429–8436 (2002).
7. V. K. Shen and J. R. Errington, *J. Phys. Chem. B* **108**, 19595–19606 (2004).
8. J. Vrabec, G. K. Kedea, G. Fuchs, and H. Hasse, *Mol. Phys.* **104**, 1509–1527 (2006).
9. T. Ikeshoji, B. Hafskjold, Y. Hashi, and Y. Kawazoe, *Phys. Rev. Lett.* **76**, 1792–1795 (1996).
10. S. Sumardiono and J. Fischer, “Molecular dynamics simulations of mixture droplet evaporation,” in *Proc. Eurotherm Seminar 77, Parma – Heat and Mass Transfer in Food Processing* (2005).
11. K. Yasuoka and M. Matsumoto, *J. Chem. Phys.* **109**, 8451–8470 (1998).
12. R. Rozas and T. Kraska, *J. Phys. Chem. C* **111**, 15784–15791 (2007).
13. M. Horsch, J. Vrabec, and H. Hasse, *Phys. Rev. E* **78**, 011603 (2008).
14. A. V. Neimark and A. Vishnyakov, *J. Phys. Chem. B* **109**, 5962–5976 (2005).
15. C. Valeriani, R. J. Allen, M. J. Morelli, D. Frenkel, and P. R. ten Wolde, *J. Chem. Phys.* **127**, 114109 (2007).
16. J. A. van Meel, A. J. Page, R. P. Sear, and D. Frenkel, *J. Chem. Phys.* **129**, 204505 (2008).
17. G. Chkonia, J. Wölk, R. Strey, J. Wedekind, and D. Reguera, *J. Chem. Phys.* **130**, 064505 (2009).
18. J. E. McDonald, *Am. J. Phys.* **31**, 31–41 (1962).
19. M. Horsch and J. Vrabec, “Grand canonical steady-state simulation of nucleation,” submitted to *J. Chem. Phys.* (2009).
20. M. M. Cielinski, M. Sc. thesis, University of Maine (1985).
21. R. Badahur and R. B. McClurg, *J. Phys. Chem. B* **105**, 11893–11900 (2001).
22. F. H. Stillinger, *J. Chem. Phys.* **38**, 1486–1494 (1963).
23. R. Zandi, D. Reguera, and H. Reiss, *J. Phys. Chem. B* **110**, 22251–22260 (2006).
24. P. G. Debenedetti, *Metastable liquids: concepts and principles*, Princeton University Press (1996).
25. D. Reguera, R. K. Bowles, Y. Djikaev, and H. Reiss, *J. Chem. Phys.* **118**, 340–353 (2003).
26. J. Wedekind, A.-P. Hyvärinen, D. Brus, and D. Reguera, *Phys. Rev. Lett.* **101**, 125703 (2008).
27. A. Laaksonen, I. J. Ford, and M. Kulmala, *Phys. Rev. E* **49**, 5517–5524 (1994).
28. M. E. Fisher, *Physics* **3**, 255 (1967).
29. B. N. Hale, *Phys. Rev. A* **33**, 4156–4163 (1986).
30. M. P. Allen and D. J. Tildesley, *Computer Simulation of Liquids*, Clarendon, Oxford (1987).
31. M. Smoluchowski, *Ann. Phys.* **25**, 205 (1908).
32. M. Smoluchowski, *Sitzungsber. Akad. Wiss. Wien* **5**, 339–368 (1915).